Supporting Information

Protein–lipid interfaces can drive the functions of membrane-embedded protein–protein complexes

Debayan Sarkar, Yashaswi Singh and Jeet Kalia*

Indian Institute of Science Education and Research (IISER) Pune

Dr. Homi Bhabha Road, Pashan, Pune–411008, Maharashtra, India.

Current address: *Department of Biological Sciences,*

Indian Institute of Science Education and Research (IISER) Bhopal

Bhopal Bypass Road, Bhauri, Bhopal–462066, Madhya Pradesh, India

*Correspondence may be addressed to:

Dr. Jeet Kalia,

Assistant Professor and Wellcome Trust-DBT India Alliance Intermediate Fellow

Tel.: +91-755-2691437; Email: jeet@iiserb.ac.in

Table of Contents

S. No.	Experimental topic/Table/Figure	Pg. No.
1	Detailed protocol for generating the interaction map of the DkTx–lipids–TRPV1 complex	3
2	Table S1: Map of interactions between DkTx and TRPV1/lipids	4-19
3	Detailed procedure for the production of DkTx and its variants	19-20
4	Figure S1: Representative DkTx purification data	20
5	Figure S2: HPLC traces for purity evaluation of all our DkTx variants	21-22
6	Electrophysiology and data analysis	23
7	Figure S3: Representative electrophysiological recordings of the DkTx variants	24-25
8	Membrane partitioning experiments on LUVs and oocytes	26
9	Figure S4: Interaction of DkTx and its variants with lipid membranes measured using tryptophan fluorescence	27
10	Figure S5: Mol. fraction partition coefficients of DkTx variants of K2 knot residues	28
11	Figure S6: Toxin depletion assays performed with DkTx and its variants	28
12	Table S2: Consolidated data summary for all DkTx variants	29
13	Figure S7: Potency (EC_{50}) vs. mol. partitioning coefficient (K_x), and Potency (EC_{50}) vs. fractional depletion plots	30
14	Structural characterization of DkTx and its variants by Circular Dichroism (CD)	30
15	Figure S8: CD spectra of DkTx and its variants	30
16	References	31

Detailed protocol for generating the interaction map of the DkTx–lipids–TRPV1 complex

The distances between the atoms of the amino acids of DkTx and those of lipid molecules/amino acids of TRPV1 were calculated by separately analyzing two pdb files of the DkTx-TRPV1 complex—one obtained from a recently published cryo-EM structure[1] and the other from a previously published docking model[2]—by using the UCSF-CHIMERA software. In this software, the command "**split**" was entered in the command line to split the PDB structure into individual peptide chains. Subsequently, each of the four monomers of the TRPV1 channel was assigned a unique model number (0, 1, 2 or 3), the two DkTx chains were assigned model numbers 4 and 5 respectively, and each of the resiniferatoxin and lipid molecules (which were present in the cryo-EM structure but not in the docking model) were assigned unique model numbers between 6 and 25. The command "**distance #a:x@ #b:y@**" was used to obtain the distance values between the amino acid residue number "x" of the DkTx chain assigned the chain model number "a" and the amino acid residue number "y" of the TRPV1 chain assigned the chain model number "b". This command yielded the distances between every possible pairs of atoms (one each belonging to the residues "x" and "y" respectively) under analysis. For every DkTx residue, this analysis was performed with respect to every amino acid residue of each of the four monomers of the channel's pore region formed by its S5, S6 and pore helices. For determining the distance between the amino acid residues of a particular DkTx chain and a lipid molecule assigned a model number "z", the command, "**distance #a:x@ #z@"** was used. This analysis was performed for every DkTx residue with respect to all the lipid molecules in the cryo-EM structure. The distance output obtained from these analyses was saved as a **"**.txt**"** file and this data was filtered manually to select for distances within the 4.4 Å cut-off distance to yield a list of TRPV1 residues/lipid molecules proximal to each DkTx residue. The resulting interaction map is depicted in Table S1 (next page).

Table S1. Map of interactions between DkTx and TRPV1/lipids.

Lipids are numbered according to the scheme employed in Figure 6 of the main text of the manuscript. The paper that reported the docking model[2] also reported MD simulations to predict lipid-interacting residues of DkTx—this information is also provided in the table below.

5irx structure[1]		Docking model[2]	
toxin residue:channel residue/lipid	distance (Å)	toxin residue:channel residue	distance (Å)
1 ASP(CB):535 LYS(NZ)	4.374		
7 GLU(N):lipid 1 6O9(H011)	4.124	Predicted as lipid-interacting (MD simulations)	
7 GLU(CA):lipid 1 6O9(N01)	3.41		
7 GLU(CA):lipid 1 ^{6}O9(H012)	3.661		
7 GLU(CA):lipid 1 6O9(H011)	2.88		
7 GLU(C):lipid 1 6O9(N01)	3.741		
7 GLU(C):lipid 1 6O9(H012)	3.627		
7 GLU(C):lipid 1 6O9(H011)	3.298		
7 GLU(CB):lipid 1 6O9(N01)	3.4		
7 GLU(CB):lipid 1 6O9(H012)	3.696		
7 GLU(CB):lipid 1 6O9(H011)	3.221		
7 GLU(CG):lipid 1 6O9(N01)	3.733		
7 GLU(CG):lipid 1 6O9(H012)	4.3		
7 GLU(CG):lipid 1 6O9(H011)	3.594		
8 VAL(N):lipid 1 6O9(N01)	3.06	Predicted as lipid-interacting (MD simulations)	
8 VAL(N):lipid 1 6O9(H012)	2.674		
8 VAL(N):lipid 1 6O9(H011)	2.815		
8 VAL(N):lipid 1 6O9(H032)	4.218		
8 VAL(CA):lipid 1 6O9(N01)	4.09		
8 VAL(CA):lipid 1 6O9(H012)	3.468		
8 VAL(CA):lipid 1 6O9(H011)	3.947		
8 VAL(C):lipid 1 6O9(H012)	4.354		
8 VAL(O):lipid 1 6O9(H012)	4.229		
8 VAL(CB):lipid 1 6O9(N01)	3.948		
8 VAL(CB):lipid 1 6O9(H012)	3.168		
8 VAL(CB):lipid 1 6O9(H011)	3.958		
8 VAL(CB):lipid 1 6O9(H032)	3.655		
8 VAL(CB):lipid 1 6O9(H101)	3.827		
8 VAL(CG1):lipid 1 6O9(H101)	3.7		
8 VAL(CG1):lipid 1 6O9(H112)	4.222		
8 VAL(CG2):lipid 1 6O9(N01)	3.763		

5irx structure[1]		Docking model[2]	
toxin residue:channel residue/lipid	distance (Å)	toxin residue:channel residue	distance (Å)
8 VAL(CG2):lipid 1 6O9(C03)	3.782		
8 VAL(CG2):lipid 1 6O9(C20)	4.395		
8 VAL(CG2):lipid 1 6O9(O22)	3.614		
8 VAL(CG2):lipid 1 6O9(H012)	3.157		
8 VAL(CG2):lipid 1 6O9(H011)	3.569		
8 VAL(CG2):lipid 1 6O9(H032)	2.903		
8 VAL(CG2):lipid 1 6O9(H031)	3.951		
8 VAL(CG2):lipid 1 6O9(H101)	3.673		
10 SER(N):653 TYR(O)	4.372	Predicted as lipid-interacting (MD simulations)	
10 SER(CA):653 TYR(O)	3.953		
10 SER(CA):655 PHE(N)	4.347		
10 SER(CA):656 LYS(N)	3.685		
10 SER(CA):656 LYS(CA)	4.242		
10 SER(CA):656 LYS(CB)	3.839		
10 SER(CA):657 ALA(N)	3.974		
10 SER(C):655 PHE(N)	3.803		
10 SER(C):655 PHE(CA)	3.89		
10 SER(C):655 PHE(C)	4.15		
10 SER(C):656 LYS(N)	3.513		
10 SER(C):656 LYS(CA)	4.377		
10 SER(C):657 ALA(N)	3.695		
10 SER(C):657 ALA(CB)	4.175		
10 SER(O):655 PHE(N)	3.604		
10 SER(O):655 PHE(CA)	3.242		
10 SER(O):655 PHE(C)	3.301		
10 SER(O):655 PHE(O)	4.309		
10 SER(O):656 LYS(N)	2.809		
10 SER(O):656 LYS(CA)	3.652		
10 SER(O):656 LYS(C)	3.616		
10 SER(O):656 LYS(CB)	4.137		
10 SER(O):657 ALA(N)	2.735		
10 SER(O):657 ALA(CA)	3.615		
10 SER(O):657 ALA(C)	4.301		
10 SER(O):657 ALA(CB)	3.488		
10 SER(O):658 VAL(N)	3.952		
10 SER(CB):656 LYS(N)	4.086		
10 SER(CB):656 LYS(CA)	4.145		
10 SER(CB):656 LYS(C)	4.141		

5irx structure[1]		Docking model[2]	
toxin residue:channel residue/lipid	distance (Å)	toxin residue:channel residue	distance (Å)
10 SER(CB):656 LYS(CB)	3.575		
10 SER(CB):656 LYS(CG)	4.285		
10 SER(CB):657 ALA(N)	3.407		
10 SER(CB):657 ALA(CA)	4.149		
10 SER(CB):657 ALA(CB)	3.78		
11 TRP(N):655 PHE(N)	4.22	Predicted as lipid-interacting (MD simulations)	
11 TRP(CA):655 PHE(N)	4.292		
11 TRP(CA):655 PHE(CA)	4.347		
11 TRP(C):655 PHE(N)	4.043		
11 TRP(C):655 PHE(CA)	4.313		
11 TRP(C):655 PHE(CG)	4.352		
11 TRP(C):655 PHE(CD1)	4.064		
11 TRP(C):655 PHE(CE1)	4.079		
11 TRP(C):655 PHE(CZ)	4.347		
11 TRP(O):655 PHE(N)	3.4	11 TRP(CA):655 PHE(N)	3.953
11 TRP(O):655 PHE(CA)	3.627	11 TRP(CA):655 PHE(CA)	4.169
11 TRP(O):655 PHE(CB)	4	11 TRP(CA):655 PHE(CD2)	4.371
11 TRP(O): 655PHE(CG)	3.213	11 TRP(C):655 PHE(N)	3.576
11 TRP(O):655 PHE(CD1)	3.028	11 TRP(C):655 PHE(CA)	4.21
11 TRP(O):655 PHE(CD2)	3.401	11 TRP(C):655 PHE(CD2)	4.305
11 TRP(O):655 PHE(CE1)	3.069	11 TRP(O):655 PHE(N)	2.94
11 TRP(O):655 PHE(CE2)	3.438	11 TRP(O):655 PHE(CA)	3.928
11 TRP(O):655 PHE(CZ)	3.256	11 TRP(O):655 PHE(CG)	4.5
11 TRP(CG):657 ALA(CB)	4.398	11 TRP(O):654 ASP(C)	3.69
11 TRP(CD1):657 ALA(CB)	3.935	11 TRP(O):654 ASP(CA)	3.488
11 TRP(CD2):657 ALA(CB)	4.217	11 TRP(O):654 ASP(CB)	3.868
11 TRP(CD2):658 VAL(CG2)	3.505	11 TRP(CG):655 PHE(CD2)	4.24
11 TRP(NE1):657 ALA(CB)	3.38	11 TRP(CD1):657 ALA(CB)	4.279
11 TRP(CE2):657 ALA(CB)	3.575	11 TRP(CD2):658 VAL(CG2)	3.941
11 TRP(CE3):657 ALA(CG2)	3.505	11 TRP(NE1):657 ALA(CB)	4.127
11 TRP(CZ2):657 ALA(CB)	3.895	11 TRP(CE3):657 ALA(CG2)	3.596
11 TRP(CZ3):658 VAL(CG2)	3.531	11 TRP(CE3):655 PHE(CD2)	4.018
11 TRP(CH2):658 VAL(CG2)	4.311	11 TRP(CE3):657 PHE(CE2)	4.252
11 TRP(CH2):661 ILE(CD2)	4.318	11 TRP(CZ3):658 VAL(CG2)	3.89
		11 TRP(CB):655 PHE(N)	4.108
		11 TRP(CB):655 PHE(CA)	3.838
		11 TRP(CB):655 PHE(CG)	4.017
		11 TRP(CB):655 PHE(CD2)	3.31

5irx structure[1]		Docking model[2]	
toxin residue:channel residue/lipid	distance (Å)	toxin residue:channel residue	distance (Å)
		11 TRP(CB):655 PHE(CE2)	3.71
11 TRP (CB): lipid 1 6O9 (H112)	3.682		
11 TRP (CG):lipid 1 6O9 (O18)	4.233		
11 TRP (CG):lipid 1 6O9 (H112)	3.841		
11 TRP (CD1):lipid 1 6O9 (H112)	4.28		
11 TRP (CD2):lipid 1 6O9 (C13)	4.054		
11 TRP (CD2):lipid 1 6O9 (O18)	3.745		
11 TRP (CD2):lipid 1 6O9 (H112)	4.289		
11 TRP (CD2):lipid 1 6O9 (H142)	4.054		
11 TRP (CD2):lipid 1 6O9 (H151)	4.183		
11 TRP (NE1):lipid 1 6O9 (H142)	4.235		
11 TRP (CE2):lipid 1 6O9 (C13)	4.337		
11 TRP (CE2):lipid 1 6O9 (C14)	4.345		
11 TRP (CE2):lipid 1 6O9 (O18)	4.369		
11 TRP (CE2):lipid 1 6O9 (H142)	3.669		
11 TRP (CE2):lipid 1 6O9 (H151)	4.324		
11 TRP (CE2):lipid 1 6O9 (H162)	4.279		
11 TRP (CE3):lipid 2 6OE (H181)	4.255		
11 TRP (CE3):lipid 1 6O9 (C13)	4.076		
11 TRP (CE3):lipid 1 6O9 (C15)	4.345		
11 TRP (CE3):lipid 1 6O9 (O18)	3.463		
11 TRP (CE3):lipid 1 6O9 (H142)	4.238		
11 TRP (CE3):lipid 1 6O9 (H151)	3.535		
11 TRP (CZ2):lipid 1 6O9 (C14)	4.215		
11 TRP (CZ2):lipid 1 6O9 (C15)	4.291		
11 TRP (CZ2):lipid 1 6O9 (C16)	4.166		
11 TRP (CZ2):lipid 1 6O9 (H142)	3.496		
11 TRP (CZ2):lipid 1 6O9 (H151)	3.916		
11 TRP (CZ2):lipid 1 6O9 (H162)	3.308		
11 TRP (CZ3): lipid 2 6OE (H181)	4.043		
11 TRP (CZ3):lipid 1 6O9 (C13)	4.373		
11 TRP (CZ3):lipid 1 6O9 (C14)	4.287		
11 TRP (CZ3):lipid 1 6O9 (C15)	3.812		
11 TRP (CZ3):lipid 1 6O9 (C16)	4.147		
11 TRP (CZ3):lipid 1 6O9 (O18)	3.878		
11 TRP (CZ3):lipid 1 6O9 (H142)	4.061		
11 TRP (CZ3):lipid 1 6O9 (H151)	2.99		
11 TRP (CZ3):lipid 1 6O9 (H162)	3.604		
11 TRP (CZ3):lipid 1 6O9 (H172)	4.294		

5irx structure[1]		Docking model[2]	
toxin residue:channel residue/lipid	distance (Å)	toxin residue:channel residue	distance (Å)
11 TRP (CH2):lipid 1 6O9 (C14)	4.176		
11 TRP CH2):lipid 1 6O9 (C15)	3.786		
11 TRP (CH2):lipid 1 6O9 (C16)	3.662		
11 TRP (CH2):lipid 1 6O9 (C17)	4.315		
11 TRP (CH2):lipid 1 6O9 (H142)	3.698		
11 TRP (CH2):lipid 1 6O9 (H151)	3.22		
11 TRP (CH2):lipid 1 6O9 (H162)	2.877		
11 TRP (CH2):lipid 1 6O9 (H172)	4.185		
12 GLY(C):535 LYS(CD)	4.24	12 GLY(O):535 LYS(CE)	4.374
12 GLY(C):654 ASP(CB)	4.333	12 GLY(O):535 LYS(NZ)	3.858
12 GLY(O):535 LYS(CG)	4.273	12 GLY(O):535 LYS(CD)	3.921
12 GLY(O):535 LYS(CD)	3.511	12 GLY(O):535 LYS(CE)	3.741
12 GLY(O):654 ASP(CA)	4.351	12 GLY(O):535 LYS(NZ)	2.894
12 GLY(O):654 ASP(CB)	3.545	12 GLY(O):654 ASP(CG)	4.02
12 GLY(O):655 PHE(CD2)	4.284	12 GLY(O):654 ASP(OD1)	4.078
12 GLY(O):655 PHE(CE2)	3.907	12 GLY(O):654 ASP(OD2)	4.156
		12 GLY(N):655 PHE(CE2)	4.312
		12 GLY(N):655 PHE(CZ)	4.382
		12 GLY(CA):535 LYS(CD)	3.84
		12 GLY(CA):535 LYS(CE)	4.085
		12 GLY(CA):535 LYS(NZ)	4.094
		12 GLY(CA):655 PHE(CZ)	4.319
13 LYS(CA):654 ASP(CB)	4.163	13 LYS(O):654 ASP(OD1)	4.219
13 LYS(C):654 ASP(CA)	4.393		
13 LYS(C):654 ASP(CB)	4.35		
14 LYS (N):654 ASP(N)	4.398	14 LYS(CD):654 ASP(OD1)	4.274
14 LYS (N):654 ASP(CA)	4.112	14 LYS(CE):654 ASP(CG)	4.244
14 LYS (N):654 ASP(CB)	4.072	14 LYS(CE):654 ASP(OD1)	3.818
14 LYS(CA):653 TYR(O)	4.36	14 LYS(CE):654 ASP(OD2)	3.823
14 LYS(CB):653 TYR(C)	3.944	14 LYS(NZ):654 ASP(CG)	3.386
14 LYS(CB):653 TYR(O)	4.015	14 LYS(NZ):652 ASP(OD1)	2.958
14 LYS (CB):654 ASP(N)	3.854	14 LYS(NZ):652 ASP(OD2)	3.129
14 LYS (CB):654 ASP(CA)	4.395	14 LYS(CG):652 ASP(OD1)	3.571
14 LYS(CE):652 ASN(C)	4.178		
14 LYS(CE):652 ASN(O)	3.653		

5irx structure[1]		Docking model[2]	
toxin residue:channel residue/lipid	distance (Å)	toxin residue:channel residue	distance (Å)
14 LYS(CE):652 ASN(CB)	3.917		
14 LYS(NZ):652 ASN(C)	4.107		
14 LYS(NZ):652 ASN(O)	3.214		
14 LYS(NZ):652 ASN(CB)	4.222		
		23 CYS(CA):656 LYS(NZ)	4.201
		23 CYS(C):656 LYS(NZ)	3.847
		23 CYS(O):656 LYS(CE)	3.623
		23 CYS(O):656 LYS(NZ)	2.861
		23 CYS(CB):656 LYS(CE)	4.304
		23 CYS(CB):656 LYS(NZ)	3.523
		23 CYS(SG):656 LYS(CE)	3.91
		23 CYS(SG):656 LYS(NZ)	3.783
25 MET(C):631 TYR(CD2)	3.843	25 MET(C):629 SER(OG)	4.384
25 MET(C):631 TYR(CE2)	4.08	25 MET(SD):648 GLU(OE2)	3.909
25 MET(O):631 TYR(CG)	4.358	25 MET(SD):650 THR(CG2)	3.822
25 MET(O):631 TYR(CD2)	3.191	25 MET(CE):635 LEU(CD1)	3.934
25 MET(O):631 TYR(CE2)	3.099	25 MET(CE):650 THR(CG2)	4.226
25 MET(O):631 TYR(CZ)	4.215	25 MET(CE):660 ILE(CG1)	4.012
25 MET(CE):635 LEU(CD1)	3.732	25 MET(N):629 SER(OG)	4.296
25 MET(CE):649 PHE(CB)	4.066	25 MET(CB):629 SER(OG)	4.005
25 MET(CE):649 PHE(CD2)	4.165	25 MET(CG):635 LEU(CD1)	4.162
25 MET(CE):660 ILE(CD1)	4.374	25 MET(CG):648 GLU(OE1)	3.394
26 GLU(N):631 TYR(CD2)	4.194	26 GLU(CA):631 TYR(CB)	3.822
26 GLU(CA):631 TYR(CB)	3.983	26 GLU(CA):631 TYR(CG)	3.605
26 GLU(CA):631 TYR(CG)	4.022	26 GLU(CA):631 TYR(CD2)	3.577
26 GLU(CA):631 TYR(CD2)	3.61	26 GLU(CA):631 TYR(CE2)	4.153
26 GLU(CA):631 TYR(CE2)	4.367	26 GLU(CA):631 TYR(CD1)	4.205
26 GLU(C):631 TYR(CG)	4.211	26 GLU(N):629 SER(OG)	4.094
26 GLU(C):631 TYR(CD2)	3.949	26 GLU(N):631 TYR(CB)	3.775
26 GLU(CB):631 TYR(CB)	4.287	26 GLU(N):631 TYR(CG)	4.102
26 GLU(CB):629 SER(CB)	4.395	26 GLU(N):631 TYR(CD2)	4.191
26 GLU(CB):629 SER(OG)	3.882	26 GLU(O):631 TYR(CD2)	4.241
		26 GLU(CG):629 SER(CB)	4.345
		26 GLU(CG):629 SER(OG)	3.585
		26 GLU(CD):629 SER(CB)	4.353
		26 GLU(CD):629 SER(OG)	3.5

5irx structure[1]		Docking model[2]	
toxin residue:channel residue/lipid	distance (Å)	toxin residue:channel residue	distance (Å)
		26 GLU(CD):630 LEU(N)	4.122
		26 GLU(CD):631 TYR(N)	3.938
		26 GLU(CD):631 TYR(CB)	4.164
		26 GLU(CD):631 TYR(CG)	3.969
		26 GLU(CD):631 TYR(CD1)	3.588
		26 GLU(CD):631 TYR(CE1)	4.165
		26 GLU(OE1):631 TYR(CG)	4.008
		26 GLU(OE1):631 TYR(CD1)	3.337
		26 GLU(OE1):631 TYR(CE1)	3.514
		26 GLU(OE1):631 TYR(CZ)	4.302
		26 GLU(OE2):629 SER(CA)	3.509
		26 GLU(OE2):629 SER(C)	3.467
		26 GLU(OE2):629 SER(OG)	4.383
		26 GLU(OE2):629 SER(CB)	3.514
		26 GLU(OE2):629 SER(OG)	2.652
		26 GLU(OE2):630 LEU(N)	2.993
		26 GLU(OE2):630 LEU(CA)	3.685
		26 GLU(OE2):630 LEU(C)	3.788
		26 GLU(OE2):630 LEU(CB)	3.874
		26 GLU(OE2):631 TYR(N)	2.973
		26 GLU(OE2):631 TYR(CA)	3.937
		26 GLU(OE2):631 TYR(CB)	3.738
		26 GLU(OE2):631 TYR(CG)	3.874
		26 GLU(OE2):631 TYR(CD1)	3.489
		26 GLU(OE2):631 TYR(CE1)	4.363
26 GLU (CA):lipid 3 6OE (O07)	3.224	Predicted as lipid-interacting (MD simulations)	
26 GLU (C):lipid 3 6OE (P05)	4.143		
26 GLU (C):lipid 3 6OE (O07)	2.638		
26 GLU (C):lipid 3 6OE (H092)	4.365		
26 GLU (O):lipid 3 6OE (O04)	4.354		
26 GLU (O):lipid 3 6OE (P05)	3.236		
26 GLU (O):lipid 3 6OE (O06)	3.752		
26 GLU (O):lipid 3 6OE (O07)	1.819		
26 GLU (O):lipid 3 6OE (O08)	4.04		
26 GLU (O):lipid 3 6OE (H092)	3.964		
26 GLU (CB):lipid 3 6OE (C03)	4.166		
26 GLU (CB):lipid 3 6OE (O04)	4.253		
26 GLU (CB):lipid 3 6OE (P05)	4.126		
26 GLU (CB):lipid 3 6OE (O07)	2.973		

5irx structure[1]		Docking model[2]	
toxin residue:channel residue/lipid	distance (Å)	toxin residue:channel residue	distance (Å)
26 GLU (CB):lipid 3 6OE (H031)	3.342		
27 PHE(N):631 TYR(CG)	4.312	27 PHE(N):631 TYR(CD2)	3.948
27 PHE(N):631 TYR(CD2)	3.796	27 PHE(N):631 TYR(CE2)	3.745
27 PHE(N):631 TYR(CE2)	3.822	27 PHE(N):631 TYR(CZ)	4.284
27 PHE(N):631 TYR(CZ)	4.351	27 PHE(CA):631 TYR(CE2)	4.228
27 PHE(CA):631 TYR(CE2)	4.141	27 PHE(CB):631 TYR(CE2)	4.387
27 PHE(CA):631 TYR(CZ)	4.215		
27 PHE(O):657 ALA(CB)	4.14		
27 PHE(CB):631 TYR(CG)	4.044		
27 PHE(CB):631 TYR(CD1)	3.756		
27 PHE(CB):631 TYR(CD2)	4.079		
27 PHE(CB):631 TYR(CE1)	3.515		
27 PHE(CB):631 TYR(CE2)	3.856		
27 PHE(CB):631 TYR(CZ)	3.563		
27 PHE(CB):631 TYR(OH)	4.065		
27 PHE(CG):631 PHE(CE1)	4.03		
27 PHE(CG):631 TYR(CZ)	4.236		
27 PHE(CG):631 TYR(OH)	4.391		
27 PHE(CD1):631 TYR(CE1)	4.125		
27 PHE(CD1):631 TYR(CZ)	4.134		
27 PHE(CD1):631 TYR(OH)	3.855		
27 PHE(CE1):661 ILE(CD1)	3.792		
27 PHE (N):lipid 3 6OE (O07)	3.71	Predicted as lipid-interacting (MD simulations)	
27 PHE (CA):lipid 3 6OE (O07)	4.244		
27 PHE (CB):lipid 3 6OE (O07)	3.89		
27 PHE (CB):lipid 3 6OE (C09)	4.25		
27 PHE (CB):lipid 3 6OE (H092)	3.33		
27 PHE (CG):lipid 3 6OE (O20)	4.227		
27 PHE (CG):lipid 3 6OE (H092)	3.837		
27 PHE (CG):lipid 3 6OE (H232)	3.635		
27 PHE (CD1):lipid 3 6OE (H232)	3.612		
27 PHE (CD1):lipid 3 6OE (H252)	3.911		
27 PHE (CD1):lipid 3 6OE (H251)	4.309		
27 PHE (CD2):lipid 3 6OE (O20)	3.807		
27 PHE (CD2):lipid 3 6OE (C21)	4.336		
27 PHE (CD2):lipid 3 6OE (H092)	3.786		
27 PHE (CD2):lipid 3 6OE (H232)	3.669		
27 PHE (CE1):lipid 3 6OE (C25)	4.306		
27 PHE (CE1):lipid 3 6OE (H232)	3.624		

5irx structure[1]		Docking model[2]	
toxin residue:channel residue/lipid	distance (Å)	toxin residue:channel residue	distance (Å)
27 PHE (CE1):lipid 3 6OE (H252)	3.517		
27 PHE (CE1):lipid 3 6OE (H251)	4.383		
27 PHE (CE2):lipid 3 6OE (O20)	4.271		
27 PHE (CE2):lipid 3 6OE (C21)	4.361		
27 PHE (CE2):lipid 3 6OE (H221)	3.949		
27 PHE (CE2):lipid 3 6OE (H232)	3.681		
27 PHE (CZ):lipid 3 6OE (H162)	4.019		
27 PHE (CZ):lipid 3 6OE (H221)	4.097		
27 PHE (CZ):lipid 3 6OE (H232)	3.66		
27 PHE (CZ):lipid 3 6OE (H252)	4.124		
28 ILE (N):lipid 3 6OE (O07)	4.21	Predicted as lipid-interacting (MD simulations)	
28 ILE (CD1):lipid 1 6O9 (O12)	4.395		
28 ILE (CD1):lipid 1 6O9 (C14)	3.91		
28 ILE (CD1):lipid 1 6O9 (H141)	3.968		
28 ILE (CD1):lipid 1 6O9 (H142)	3.078		
30 HIS		Predicted as lipid-interacting (MD simulations)	
43 ASN(O):535 LYS(NZ)	4.322	43 ASN(OD1):535 LYS(NZ)	4.343
43 ASN(CB):535 LYS(NZ)	3.708	43 ASN(ND2):654 ASP(CG)	3.832
		43 ASN(ND2):654 ASP(OD1)	4.275
		43 ASN(ND2):654 ASP(OD2)	3.228
49 GLU (CA):lipid 4 6O9 (N01)	3.756	Predicted as lipid-interacting (MD simulations)	
49 GLU (CA):lipid 4 6O9 (H012)	4.192		
49 GLU (CA):lipid 4 6O9 (H011)	3.126		
49 GLU (C):lipid 4 6O9 (N01)	3.955		
49 GLU (C):lipid 4 6O9 (H012)	4.074		
49 GLU (C):lipid 4 6O9 (H011)	3.359		
49 GLU (CB):lipid 4 6O9 (N01)	3.792		
49 GLU (CB):lipid 4 6O9 (H012)	4.266		
49 GLU (CB):lipid 4 6O9 (H011)	3.473		
49 GLU (CG):lipid 4 6O9 (N01)	4.167		
49 GLU (CG):lipid 4 6O9 (H011)	3.936		
50 VAL (N):lipid 4 6O9 (N01)	3.15	Predicted as lipid-interacting (MD simulations)	
50 VAL (N):lipid 4 6O9 (H012)	3.03		
50 VAL (N):lipid 4 6O9 (H011)	2.705		

5irx structure[1]		Docking model[2]	
toxin residue:channel residue/lipid	distance (Å)	toxin residue:channel residue	distance (Å)
50 VAL (CA):lipid 4 6O9 (N01)	4.093		
50 VAL (CA):lipid 4 6O9 (H012)	3.683		
50 VAL (CA):lipid 4 6O9 (H011)	3.771		
50 VAL (CB):lipid 4 6O9 (N01)	3.84		
50 VAL (CB):lipid 4 6O9 (O06)	4.338		
50 VAL (CB):lipid 4 6O9 (H012)	3.179		
50 VAL (CB):lipid 4 6O9 (H011)	3.71		
50 VAL (CB):lipid 4 6O9 (H032)	3.986		
50 VAL (CB):lipid 4 6O9 (H101)	3.744		
50 VAL (CG1):lipid 4 6O9 (H101)	3.719		
50 VAL (CG1):lipid 4 6O9 (H112)	4.041		
50 VAL (CG2):lipid 4 6O9 (N01)	3.66		
50 VAL (CG2):lipid 4 6O9 (C03)	4.017		
50 VAL (CG2):lipid 4 6O9 (O06)	4.276		
50 VAL (CG2):lipid 4 6O9 (C10)	4.326		
50 VAL (CG2):lipid 4 6O9 (C20)	4.259		
50 VAL (CG2):lipid 4 6O9 (O22)	3.538		
50 VAL (CG2):lipid 4 6O9 (H012)	3.113		
50 VAL (CG2):lipid 4 6O9 (H011)	3.369		
50 VAL (CG2):lipid 4 6O9 (H032)	3.094		
50 VAL (CG2):lipid 4 6O9 (H031)	4.37		
50 VAL (CG2):lipid 4 6O9 (H101)	3.372		
		51 CYS(SG):656 LYS(CE)	4.227
52 GLY(N):653 TYR(O)	4.348	52 GLY(C):655 PHE(N)	3.692
52 GLY(CA):653 TYR(O)	3.965	52 GLY(C):655 PHE(CA)	4.042
52 GLY(CA):656 LYS(N)	3.767	52 GLY(C):654 ASP(OD1)	4.221
52 GLY(CA):656 LYS(CA)	4.307	52 GLY(O):655 PHE(CA)	3.398
52 GLY(CA):656 LYS(CB)	3.872	52 GLY(O):655 PHE(C)	4.291
52 GLY(CA):657 ALA(N)	4.045	52 GLY(O):656 LYS(N)	4.137
52 GLY(C):655 PHE(N)	3.846	52 GLY(O):654 ASP(CA)	3.973
52 GLY(C):655 PHE(CA)	3.945	52 GLY(O):654 ASP(C)	3.797
52 GLY(C):655 PHE(C)	4.177	52 GLY(O):654 ASP(CG)	4.139
52 GLY(C):656 LYS(N)	3.509	52 GLY(O):654 ASP(OD1)	3.034
52 GLY(C):656 LYS(CA)	4.349	52 GLY(O):654 ASP(N)	2.753
52 GLY(C):657 ALA(N)	3.676		
52 GLY(C):657 ALA(CB)	4.163		
52 GLY(O):655 PHE(N)	3.596		

5irx structure[1]		Docking model[2]	
toxin residue:channel residue/lipid	distance (Å)	toxin residue:channel residue	distance (Å)
52 GLY(O):655 PHE(CA)	3.261		
52 GLY(O):655 PHE(C)	3.275		
52 GLY(O):655 PHE(O)	4.291		
52 GLY(O):656 LYS(N)	2.73		
52 GLY(O):656 LYS(CA)	3.552		
52 GLY(O):656 LYS(C)	3.54		
52 GLY(O):656 LYS(CB)	4.007		
52 GLY(O):657 ALA(N)	2.677		
52 GLY(O):657 ALA(CA)	3.594		
52 GLY(O):657 ALA(C)	4.319		
52 GLY(O):657 ALA(CB)	3.49		
52 GLY(O):658 VAL(N)	3.995		
53 TRP(N):655 PHE(N)	4.28	53 TRP(CA):655 PHE(CD2)	4.174
53 TRP(CA):655 PHE(N)	4.329	53 TRP(C):655 PHE(CD2)	3.717
53 TRP(CA):655 PHE(CA)	4.27	53 TRP(C):655 PHE(CE2)	3.72
53 TRP(C):655 PHE(N)	4.032	53 TRP(O):655 PHE(CD1)	3.523
53 TRP(C):655 PHE(CA)	4.272	53 TRP(O):655 PHE(CE2)	3.2
53 TRP(C):655 PHE(CG)	4.364	53 TRP(O):655 PHE(CZ)	4.182
53 TRP(C):655 PHE(CD1)	4.065	53 TRP(O):636 GLU(CG)	4.113
53 TRP(C):655 PHE(CE1)	4.112	53 TRP(CD1):657 ALA(CB)	4.117
53 TRP(O):655 PHE(N)	3.373	53 TRP(CD2):657 ALA(CB)	4.02
53 TRP(O):655 PHE(CA)	3.56	53 TRP(CD2):658 VAL(CG2)	
53 TRP(O):655 PHE(CB)	3.961	53 TRP(NE1):657 ALA(CB)	3.472
53 TRP(O):655 PHE(CG)	3.209	53 TRP(CE2):657 ALA(CB)	3.396
53 TRP(O):655 PHE(CB)	3.004	53 TRP(CE3):658 VAL(CG2)	3.646
53 TRP(O):655 PHE(CD1)	3.454	53 TRP(CZ2):657 ALA(CB)	3.538
53 TRP(O):655 PHE(CD2)	3.089	53 TRP(CZ3):658 VAL(CG2)	3.495
53 TRP(O):655 PHE(CE2)	3.528	53 TRP(CH2):658 VAL(CG2)	4.305
53 TRP(O):655 PHE(CZ)	3.332	53 TRP(CH2):661 ILE(CD1)	3.982
53 TRP(CG):657 ALA(CB)	4.328	53 TRP(CH2):657 ALA(CB)	4.256
53 TRP(CD1):657 ALA(CB)	3.895		
53 TRP(CD2):657 ALA(CB)	4.166		
53 TRP(CD2):658 VAL(CG2)	4.305		
53 TRP(NE1):657 ALA(CB)	3.39		
53 TRP(CE2):657 ALA(CB)	3.576		
53 TRP(CE3):658 VAL(CG2)	3.52		
53 TRP(CZ2):657 ALA(CB)	3.931		
53 TRP(CZ3):658 VAL(CG2)	3.568		
53 TRP(CH2):658 VAL(CG2)	4.382		

5irx structure[1]		Docking model[2]	
toxin residue:channel residue/lipid	distance (Å)	toxin residue:channel residue	distance (Å)
53 TRP(CH2):661 ILE(CD1)	4.28		
53 TRP (CB):lipid 4 6O9 (H112)	3.837	Predicted as lipid-interacting (MD simulations)	
53 TRP (CG):lipid 4 6O9 (O18)	4.372		
53 TRP (CG):lipid 4 6O9 (H112)	3.959		
53 TRP (CD1):lipid 4 6O9 (H112)	4.371		
53 TRP (CD2):lipid 4 6O9 (C13)	4.206		
53 TRP (CD2):lipid 4 6O9 (O18)	3.863		
53 TRP (CD2):lipid 4 6O9 (H112)	4.37		
53 TRP (CD2):lipid 4 6O9 (H142)	4.238		
53 TRP (CD2):lipid 4 6O9 (H151)	4.385		
53 TRP (NE1):lipid 4 6O9 (H142)	4.33		
53 TRP (CE2):lipid 4 6O9 (H142)	3.809		
53 TRP (CE2):lipid 4 6O9 (H162)	4.34		
53 TRP (CE3):lipid 4 6O9 (C13)	4.252		
53 TRP (CE3):lipid 4 6O9 (O18)	3.609		
53 TRP (CE3):lipid 4 6O9 (H151)	3.8		
53 TRP (CE3):lipid 5 6OE (H181)	4.36		
53 TRP (CZ2):lipid 4 6O9 (C14)	4.324		
53 TRP (CZ2):lipid 4 6O9 (C15)	4.395		
53 TRP (CZ2):lipid 4 6O9 (C16)	4.237		
53 TRP (CZ2):lipid 4 6O9 (H142)	3.623		
53 TRP (CZ2):lipid 4 6O9 (H151)	4.027		
53 TRP (CZ2):lipid 4 6O9 (H162)	3.369		
53 TRP (CZ3):lipid 4 6O9 (C15)	4.058		
53 TRP (CZ3):lipid 4 6O9 (C16)	4.356		
53 TRP (CZ3):lipid 4 6O9 (O18)	3.964		
53 TRP (CZ3):lipid 4 6O9 (H142)	4.268		
53 TRP (CZ3):lipid 4 6O9 (H151)	3.249		
53 TRP (CZ3):lipid 4 6O9 (H162)	3.764		
53 TRP (CZ3):lipid 4 6O9 (H181)	4.071		
53 TRP (CH2):lipid 4 6O9 (C14)	4.326		
53 TRP (CH2):lipid 4 6O9 (C15)	3.95		
53 TRP (CH2):lipid 4 6O9 (C16)	3.808		
53 TRP (CH2):lipid 4 6O9 (H142)	3.86		
53 TRP (CH2):lipid 4 6O9 (H151)	3.384		
53 TRP (CH2):lipid 4 6O9 (H162)	3.001		
53 TRP (CH2):lipid 4 6O9 (H172)	4.324		
54 GLY(C):654 ASP(CB)	4.365	54 GLY(C):654 ASP(CG)	4.043

5irx structure[1]		Docking model[2]	
toxin residue:channel residue/lipid	distance (Å)	toxin residue:channel residue	distance (Å)
54 GLY(O):535 LYS(CD)	3.748	54 GLY(C):654 ASP(OD1)	3.313
54 GLY(O):654 ASP(CA)	4.381	54 GLY(C):654 ASP(OD2)	4.097
54 GLY(O):654 ASP(CB)	3.601	54 GLY(O):654 ASP(CG)	3.274
54 GLY(O):655 PHE(CD2)	4.202	54 GLY(O):654 ASP(OD1)	2.877
54 GLY(O):655 PHE(CE2)	3.813	54 GLY(O):654 ASP(OD2)	3.072
54 GLY(O):655 PHE(CZ)	4.307	54 GLY(N):654 ASP(OD2)	3.735
		54 GLY(N):655 PHE(CD2)	4.245
		54 GLY(N):655 PHE(CE2)	4.143
		54 GLY(CA):654 ASP(OD1)	3.683
		54 GLY(CA):655 PHE(CE2)	3.909
		54 GLY(CA):655 PHE(CZ)	4.109
55 SER(CA):654 ASP(CB)	4.147	55 SER(C):654 ASP(OD1)	4.257
55 SER(C):654 ASP(CA)	4.145	55 SER(O):654 ASP(CA)	4.258
55 SER(C):654 ASP(CB)	4.074	55 SER(O):654 ASP(CG)	3.897
		55 SER(O):654 ASP(OD1)	3.342
		55 SER(N):654 ASP(OD1)	4.082
56 LYS(N):654 LYS(N)	4.35		
56 LYS(N):654 LYS(CA)	4.043		
56 LYS(N):654 LYS(CB)	3.885		
56 LYS(CA):654 ASP(N)	4.344		
56 LYS(CG):653 TYR(C)	3.924		
56 LYS(CG):654 ASP(N)	3.414		
56 LYS(CG):654 ASP(CA)	4.126		
56 LYS(CG):654 ASP(CB)	4.115		
56 LYS(CE):652 ASN(O)	4.399		
56 LYS(CE):654 ASP(N)	4.283		
		63 CYS(CB):656 LYS(NZ)	4.339
		63 CYS(SG):656 LYS(CE)	3.937
		63 CYS(SG):656 LYS(NZ)	3.905
64 PRO(O):656 LYS(CE)	3.623	64 PRO(O):656 LYS(CE)	4.293
		64 PRO(O):656 LYS(CE)	4.06
65 LEU(O):632 SER(CB)	4.338	65 LEU(O):631 TYR(CD2)	3.642
65 LEU(CB):632 SER(CB)	4.383	65 LEU(O):631 TYR(CE2)	3.638
65 LEU(CG):632 SER(CA)	4.386	65 LEU(O):635 LEU(CD1)	4.074

5irx structure[1]		Docking model[2]	
toxin residue:channel residue/lipid	distance (Å)	toxin residue:channel residue	distance (Å)
65 LEU(CG):632 SER(CB)	3.947	65 LEU(CB):650 THR(CG2)	4.38
65 LEU(CD1):635 LEU(CD1)	4.301	65 LEU(CG):635 LEU(CD1)	3.933
65 LEU(CD1):660 ILE(CD1)	3.747	65 LEU(CG):650 THR(CG2)	4.215
65 LEU(CD2):632 SER(CA)	4.163	65 LEU(CD1):650 THR(CG2)	3.803
65 LEU(CD2):632 SER(CB)	3.663	65 LEU(CD1):656 LYS(O)	4.395
		65 LEU(CD1):657 ALA(CA)	4.186
		65 LEU(CD1):660 ILE(CG1)	3.824
		65 LEU(CD2):635 LEU(CD1)	3.594
		65 LEU(CD2):648 GLU(CB)	4.017
		65 LEU(CD2):648 GLU(CG)	3.754
		65 LEU(CD2):648 GLU(CD)	4.045
		65 LEU(CD2):648 GLU(OE1)	3.419
		65 LEU(CD2):650 THR(CG2)	3.825
		65 LEU(CD2):660 ILE(CG1)	4.235
66 ALA (CA):lipid 6 6OE (O07)	3.781	66 ALA(CA):631 TYR(CD2)	3.785
66 ALA (C):lipid 6 6OE (O07)	3.886	66 ALA(CA):631 TYR(CE2)	4.135
66 ALA (CB):lipid 6 6OE (O07)	3.295	66 ALA(O):657 ALA(CB)	4.028
		66 ALA(CB):631 TYR(CD2)	3.803
		Predicted as lipid-interacting (MD simulations)	
67 PHE(N):631 TYR(CB)	4.371	67 PHE(CE1):631 TYR(CE2)	3.901
67 PHE(N):631 TYR(CG)	3.817	67 PHE(CE1):631 TYR(CZ)	3.688
67 PHE(N):631 TYR(CD1)	4.164	67 PHE(CE1):631 TYR(OH)	4.224
67 PHE(N):631 TYR(CD2)	3.661	67 PHE(CZ):631 TYR(CE1)	4.027
67 PHE(N):631 TYR(CE1)	4.362	67 PHE(CZ):631 TYR(CE2)	4.365
67 PHE(N):631 TYR(CE2)	3.879	67 PHE(CZ):631 TYR(CZ)	3.88
67 PHE(N):631 TYR(CZ)	4.219	67 PHE(CZ):631 TYR(OH)	3.95
67 PHE(CA):631 TYR(CD1)	4.382		
67 PHE(CA):631 TYR(CD2)	4.373		
67 PHE(CA):631 TYR(CE1)	4.216		
67 PHE(CA):631 TYR(CE2)	4.204		
67 PHE(CA):631 TYR(CZ)	4.117		
67 PHE(O):657 ALA(CB)	3.653		
67 PHE(CB):631 TYR(CD1)	4.069		
67 PHE(CB):631 TYR(CE1)	4.006		
67 PHE(CB):631 TYR(CZ)	4.384		
67 PHE(CD1):631 TYR(CE1)	4.04		
67 PHE(CD1):631 TYR(CZ)	4.348		

5irx structure[1]		Docking model[2]	
toxin residue:channel residue/lipid	distance (Å)	toxin residue:channel residue	distance (Å)
67 PHE(CD1):631 TYR(OH)	4.24		
67 PHE(CE1):661 ILE(CD1)	3.922		
67 PHE (N):lipid 6 6OE (O07)	3.03	Predicted as lipid-interacting (MD simulations)	
67 PHE (N):lipid 6 6OE (H092)	3.986		
67 PHE (CA):lipid 6 6OE (O07)	3.961		
67 PHE (CA):lipid 6 6OE (H092)	4.227		
67 PHE (CB):lipid 6 6OE (O07)	3.83		
67 PHE (CB):lipid 6 6OE (O08)	4.159		
67 PHE (CB):lipid 6 6OE (C09)	4.05		
67 PHE (CB):lipid 6 6OE (O20)	4.037		
67 PHE (CB):lipid 6 6OE (H092)	3.241		
67 PHE (CB):lipid 6 6OE (H232)	4.035		
67 PHE (CG):lipid 6 6OE (O20)	4.277		
67 PHE (CG):lipid 6 6OE (H092)	4.262		
67 PHE (CG):lipid 6 6OE (H232)	3.584		
67 PHE (CD1):lipid 6 6OE (C23)	4.18		
67 PHE (CD1):lipid 6 6OE (C25)	4.223		
67 PHE (CD1):lipid 6 6OE (H232)	3.247		
67 PHE (CD1):lipid 6 6OE (H252)	3.575		
67 PHE (CD1):lipid 6 6OE (H251)	4.095		
67 PHE (CD2):lipid 6 6OE (H232)	4.217		
67 PHE (CE1):lipid 6 6OE (C24)	4.5		
67 PHE (CE1):lipid 6 6OE (C25)	4.143		
67 PHE (CE1):lipid 6 6OE (H232)	3.641		
67 PHE (CE1):lipid 6 6OE (H241)	4.246		
67 PHE (CE1):lipid 6 6OE (H252)	3.308		
67 PHE (CE1):lipid 6 6OE (H251)	4.32		
67 PHE (CE2):lipid 4 6O9 (C16)	4.063		
67 PHE (CE2):lipid 4 6O9 (H161)	3.713		
67 PHE (CE2):lipid 4 6O9 (H162)	3.502		
67 PHE (CZ):lipid 4 6O9 (C16)	4.106		
67 PHE (CZ):lipid 4 6O9 (H161)	4.025		
67 PHE (CZ):lipid 4 6O9 (H162)	3.416		
67 PHE (CZ):lipid 6 6OE (H232)	4.267		
67 PHE (CZ):lipid 6 6OE (H252)	4.28		
68 ILE (N):lipid 6 6OE (O07)	4.265	Predicted as lipid-interacting (MD simulations)	
68 ILE (CG1):lipid 4 6O9 (H142)	3.627		
68 ILE (CD1):lipid 4 6O9 (C14)	4.191		

5irx structure[1]		Docking model[2]	
toxin residue:channel residue/lipid	distance (Å)	toxin residue:channel residue	distance (Å)
68 ILE (CD1):lipid 4 6O9 (H141)	3.864		
68 ILE (CD1):lipid 4 6O9 (H142)	3.606		
70 TYR (OH):lipid 4 6O9 (H212)	3.565	Predicted as lipid-interacting (MD simulations)	

Detailed procedure for the production of DkTx and its variants

Mutagenesis and cloning:

DkTx variants were generated by performing whole-plasmid PCR on a plasmid provided by Dr. Kenton Swartz' laboratory at the NIH that contained the DkTx gene downstream of the keto-steroid isomerase (KSI) gene in a pET31b vector[3]. PCR products were digested with *Dpn I* to remove methylated parental plasmid and the digested reaction mixture was transformed into *E. coli* NEB Turbo chemically competent cells.

Transformation and linear protein preparation:

Mutant DkTx clones were confirmed by sending sequencing samples to 1st Base, Malaysia. Positive clones were transformed into chemically competent *E. coli* BL21 (DE3) cells. LB broth cultures (1 L) containing ampicillin (100 µg/mL) were inoculated with transformed *E. coli* BL21 (DE3) cells and induced with IPTG (0.5 mM) on reaching an O.D. (600 nm) of 0.4-0.6 at 37ºC. The induced culture was pelleted after 6 h of growth and lysed by sonication in Tris-HCl buffer (20 mM at pH 8.0). The sonicated cell lysate was first centrifuged at 12000 rpm for 1 h and the pellet was dissolved in guanidine hydrochloride solution (6 M), supplemented with L-methionine (67 mM). Fusion protein cleavage was performed by adding the cell lysate to a solution of hydroxylamine hydrochloride (2 M at pH 9) and incubating the resulting mixture at 45ºC for 4.5 h. Subsequently, dithiothreitol (66 mM) was added and the resulting mixture was incubated at 45ºC for 1 h for performing protein denaturation. This solution was then titrated with conc. HCl to pH 4 and centrifuged to obtain the denatured proteins in the supernatant. Subsequently, the protein solution was dialyzed against water containing 0.1% TFA and then filtered through 0.45 µm syringe filters and lyophilized to yield the linear protein as a white powder.

Refolding of linear DkTx variants:

The lyophilized linear protein was dissolved in 50% acetonitrile containing 0.1% TFA at a concentration of 2 mg/mL. This protein solution was then added to a redox refolding buffer containing Tris-HCl (0.4 M), EDTA (1 mM), Triton X-100 (0.5%), GSH (2.5 mM), GSSG (0.25 mM) at pH 8.0 and incubated at 4ºC for 2 d. Poorly folding DkTx variants, W53A, W53L and G52A required prolonged incubation of 14 d in the refolding buffer to give good yields. The progression of refolding was assessed by subjecting the refolding cocktail to analytical RP-HPLC on a C18 column (300 Å pore size) with a linear acetonitrile-water (0.1% TFA) gradient (5-65% acetonitrile over 30 min). Once refolded optimally, the refolding cocktail was titrated to pH 4 with conc. HCl to quench the refolding reaction. The refolding cocktail was then

concentrated in a 3500 MWCO dialysis membrane (Thermo Fischer Inc.) against 400 g/L solution of PEG20. The refolded DkTx variants were then purified from the concentrated refolding cocktail by RP-HPLC on a C18 column (300 Å pore size) with a linear acetonitrile-water (0.1% TFA) gradient (5-65% acetonitrile over 30 min). Purified fractions were quantified by spectrophotometric analysis from the absorbance at 280 nm and then aliquoted in 1 nmol aliquots or 4 nmol aliquots, vacuum-dried and stored at -80^{o}C until use for electrophysiological activity assays and partitioning experiments, respectively. Figure S1 depicts representative protein production data and Figure S2 depicts the purity evaluation HPLC runs for all variants. Wild-type and all DkTx variants had an additional glycine residue at their *N*-termini and three additional residues (HYR) in the linker region. The sequence of DkTx referred to as "wild-type" in the manuscript, therefore, is as follows:

GDCAKEGEVCSWGKKCCDLDNFYCPMEFIPHCKKYKPYVPVTTHYRNCAKEGEVCGW
GSKCCHGLDCPLAFIPYCEKYR

Figure S1. Representative DkTx purification data.

DkTx variants were produced as described above (pg. 19-20). The band for the overexpressed DkTx-KSI fusion protein (depicted by an asterisk in the gel picture below) was expected at 24 kDa. Gel lanes have been labeled as followed: I: induced; UI: uninduced; M: molecular weight markers; P: DkTx protein purified by HPLC after refolding (expected at 9 kDa). The red arrow below denotes the peak for the correctly folded toxin in the HPLC chromatogram.

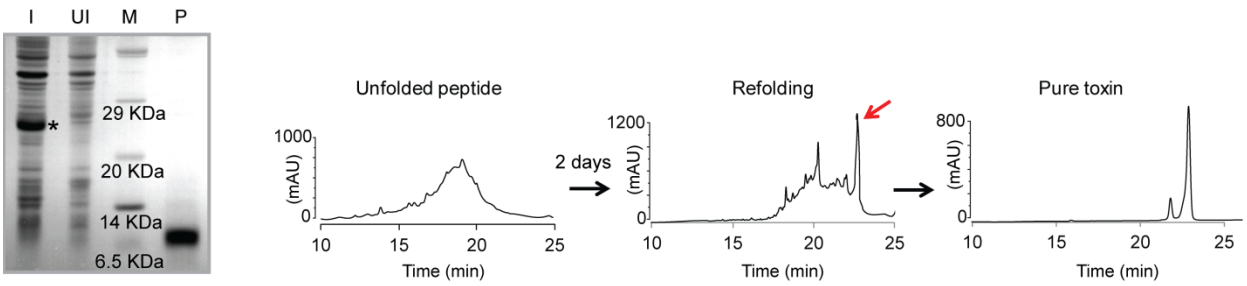

Figure S2. HPLC traces for purity evaluation of all our DkTx variants. The absorbance has been measured at 280 nm.

M25A DkTx

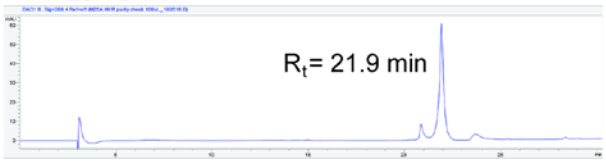

L65A DkTx

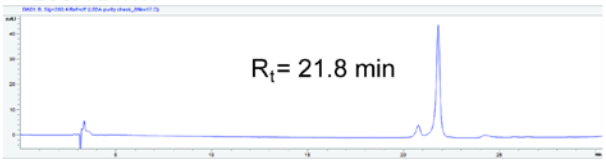

E26A DkTx

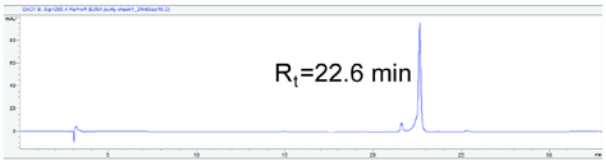

A66S DkTx

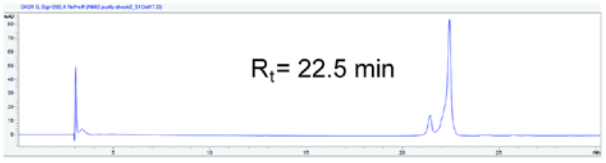

F27A DkTx

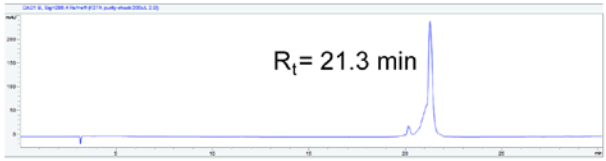

F67A DkTx

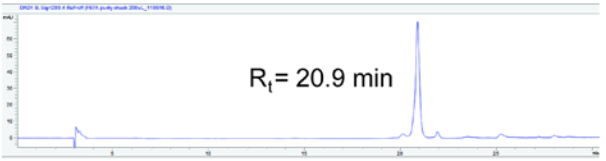

I28A DkTx

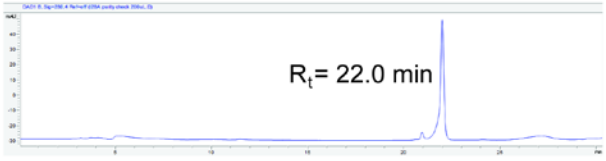

I68A DkTx

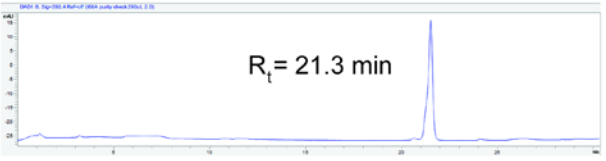

H30A DkTx

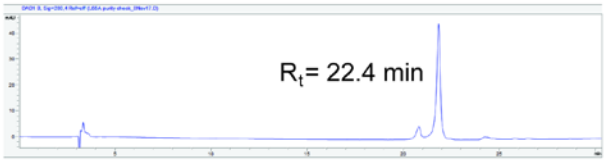

Y70A DkTx

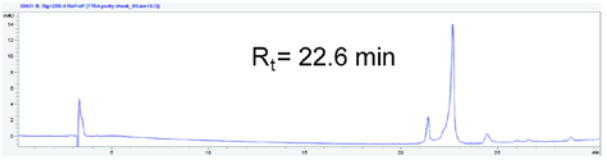

W11L DkTx

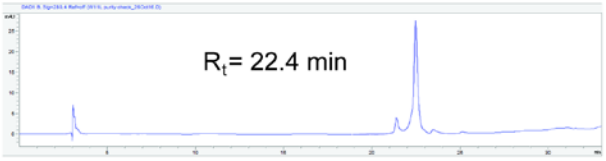

W53L DkTx

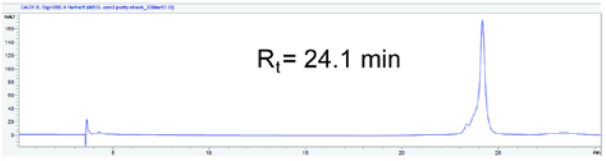

W11Y DkTx

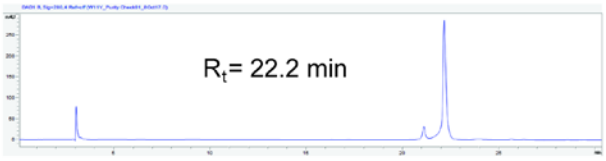

W53Y DkTx

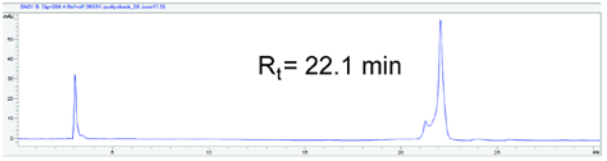

P64A DkTx

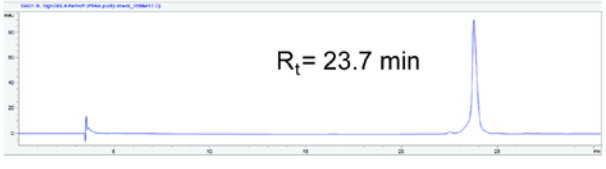

Electrophysiology and data analysis

Activity assays on DkTx variants by Two-Electrode Voltage Clamp recordings:

Stage 5 and 6 oocytes from adult female *Xenopus laevis* (the African clawed frog) were surgically removed from anesthetized frogs in accordance with a protocol approved by the Institutional Animal Ethics Committee (IAEC), IISER Pune. Oocytes were digested with collagenase type 2 enzyme (2 mg/mL) in calcium-free OR2 buffer containing NaCl (82.5 mM), KCl (2.5 mM), $MgCl_2$ (1 mM) and HEPES (5 mM) at pH 7.6 for 1 h at 18^{o}C on an automated rocker and then de-folliculated with cut pipettes. Rat TRPV1 gene cloned in pGEM-HE vector was used to make TRPV1 cRNA by *in vitro* transcription using HiScribe T7 ARCA mRNA Kit (New England Biolabs Inc.) followed by plasmid linearization by *Not I* (New England Biolabs Inc.). De-folliculated oocytes were injected with rTRPV1 cRNA solution (50 nL) in different dilutions (full strength to 1:4 dilution with RNase-free water) and stored at 18^{o}C in ND96 solution containing NaCl (96 mM), KCl (2 mM), HEPES (5 mM), $MgCl_2$ (1 mM), $CaCl_2$(1.8 mM) and gentamycin (50 µg/mL) at pH 7.6. TRPV1 channel recordings were performed on oocytes 1-2 d post-mRNA injection under voltage-clamp conditions by using a two-electrode voltage clamp instrument (Warner Instruments) in a 150 µL recording chamber. The recorded data were filtered and digitized at 0.5 KHz and 2.5 KHz respectively using digidata analog to digital converter and pClamp software (Molecular Devices). Recording microelectrode resistances were between at 0.1-1 MΩ when filled with 3 M KCl solution. The recording buffer contained NaCl (50 mM), KCl (50 mM), $MgCl_2$ (1 mM), $BaCl_2$ (0.3 mM) and HEPES (20 mM) at pH 7.4. Oocytes were held at -60 mV during recording and activated by perfusing capsaicin (5 µM in recording buffer), and following complete capsaicin wash-off, different concentrations of the wild-type/variant toxins were pipetted into the recording chamber to trigger toxin-mediated channel activation. The normalized ratios of the toxin-evoked and capsaicin-evoked peak currents were plotted to generate dose response curves. For each concentration of toxin sampling was done at least 3 times.

Dose-response plots:

The normalized ratio of toxin-induced current to that of the capsaicin current was plotted against the concentration of the toxin and the Hill equation (below) was fit to the data using Origin 9.0:

$$y = A_{max} \{(x^n)/(k^n+x^n)\}$$

where A_{max} is the normalized maximum I(toxin)/I(5 µM Capsaicin) ratio, k is EC_{50} and n is the Hill coefficient.

Data analysis to obtain toxin wash-off kinetic plots depicted in Figures 3b (middle panel) and 3c (top panel):

Electrophysiological recordings were used to extract the wash-off traces for 3 or 5 min in axon test file (.atf) format using the "Clampfit 10.5" software. The extracted traces were subjected to data point extraction at every 7500th point interval using the R3.4.1 package and the extracted points from 3-5 normalized traces were used to obtain averaged representative traces for wash-off kinetic plots along with their respective standard deviation values (error bars).

Figure S3. Representative electrophysiological recordings of the DkTx variants. All traces depicted below were obtained by applying 6.6 μM of toxin (unless otherwise mentioned).

a. Representative current traces for variants of exclusively channel-interacting DkTx residues

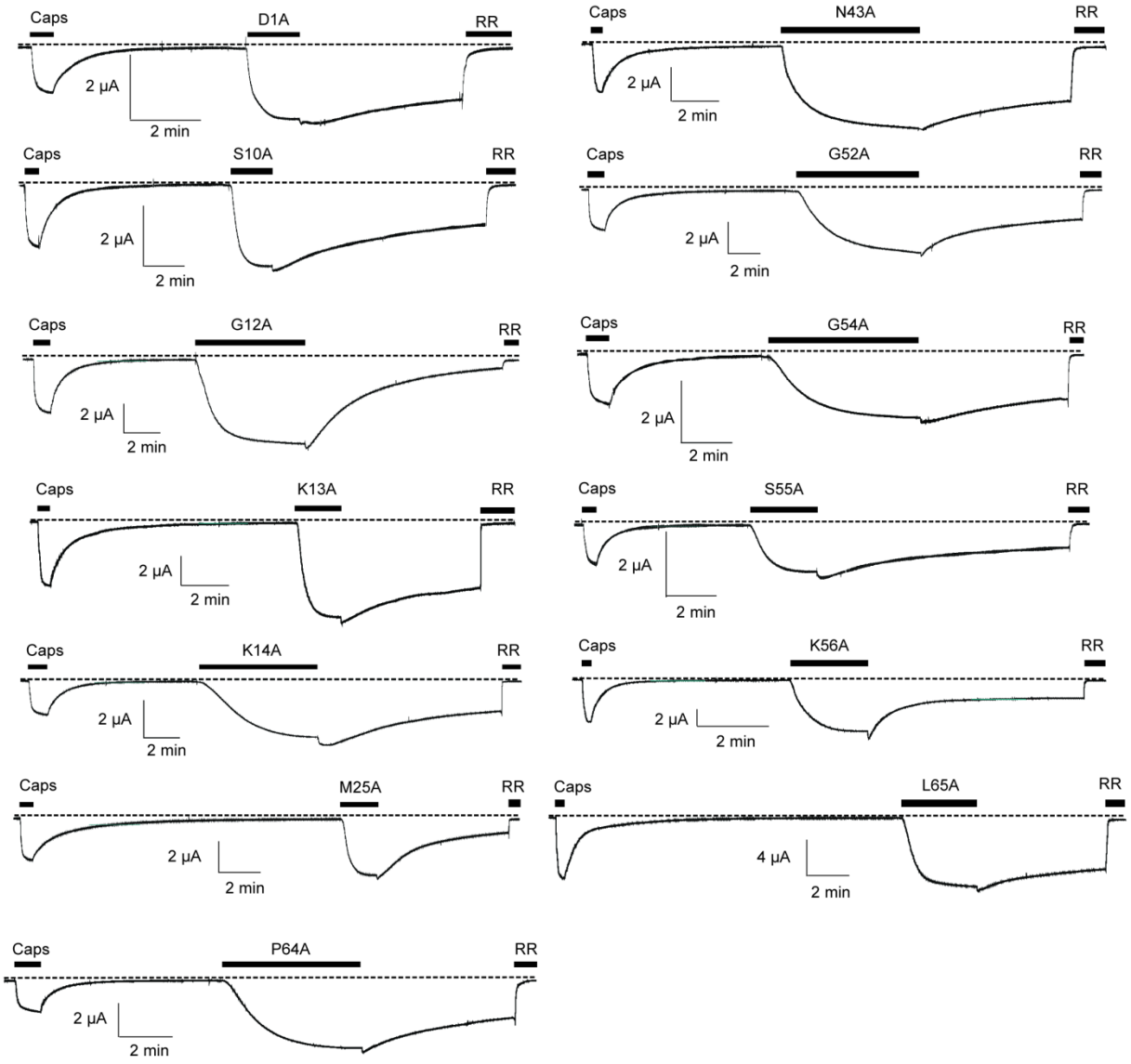

b. Representative current traces for variants of lipid-interacting DkTx residues

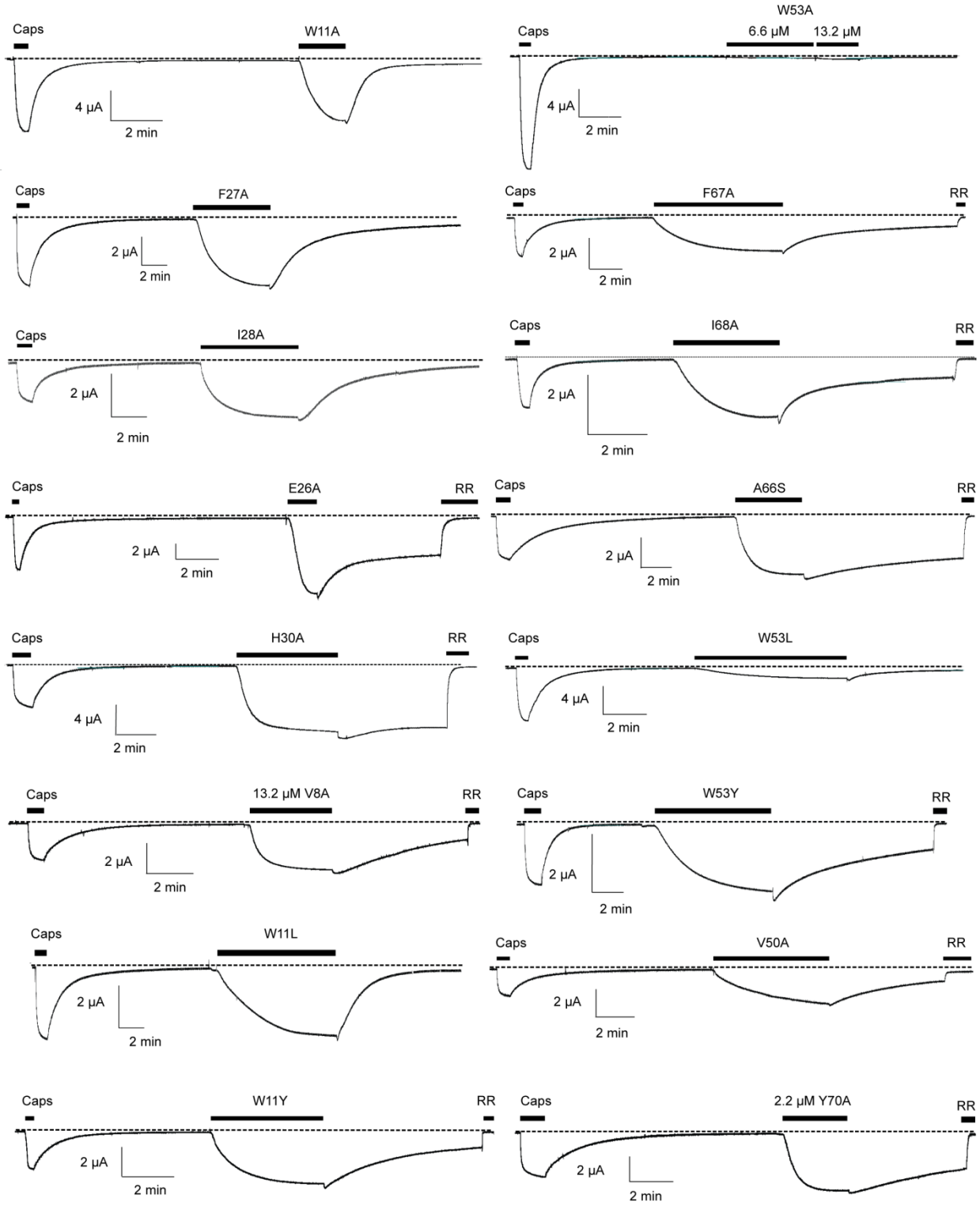

Membrane partitioning experiments on LUVs and oocytes

a) Fluorescence-based experiments on large unilamellar lipid vesicles (LUVs):

LUV preparation: 1-palmitoyl-2-oleoyl-*sn*-glycero-3-phosphocholine (16:0-18:1 PC from Avanti Polar Lipids Inc.) and 1-palmitoyl-2-oleoyl-*sn*-glycero-3-phospho-(1'-*rac*-glycerol) (sodium salt) (16:0-18:1 PG from Avanti Polar Lipids Inc.) were mixed at a molar ratio of 1:1 from their chloroform stock solutions, dried under a gentle nitrogen stream and kept in a vacuum desiccator for 9 h. Dried lipid films were rehydrated in HEB buffer at pH 7.0 containing HEPES (10 mM) and EDTA (1 mM). The resulting solution was extruded through 100 nm pore-sized polycarbonate filters (Avanti Polar Lipids Inc.) to generate LUVs.

Tryptophan fluorescence spectroscopy: DkTx variants were dissolved in 2 mL of a buffer containing HEPES (10 mM) and EDTA (1 mM) at pH 7.0 to a concentration of 2 μM and the resulting solution was excited with 280 nm wavelength light by using a Horiba FluoroMax 4 spectrofluorometer. Emission spectra were recorded between 300 to 450 nm both in the presence and absence of LUVs. Scattering of light from lipid vesicles was corrected following earlier reported methods[4,5] and the data was subjected to a fitting analysis by employing the following equation:

$$F/F_0(L) = 1+(F/F_0^{max}-1)K_x[L]/([W]+K_x[L])$$

where F is the fluorescence intensity at 320 nm for a given lipid concentration, F_0 is the fluorescence intensity at 320 nm in absence of lipids, F_0^{max} is fluorescence intensity at 320 nm at a concentration of lipids where partitioning saturates, [L] is molar concentration of accessible lipid (60% of total lipid, corresponding to the outer leaflet), [W] is molar concentration of water (55.3 M), and K_x is mole-fraction partition coefficient of the DkTx variants.

b) Toxin depletion experiments on *Xenopus laevis* oocytes:

Our toxin-depletion experiments involved incubation of 100 defolliculated stage 5 or 6 oocytes with 4 nmol of DkTx or its variants in 400 μL (final volume) of 20 mM HEPES buffer at pH 7.4 containing NaCl (50 mM), KCl (50 mM), $MgCl_2$ (1 mM) and $BaCl_2$ (0.3 mM) for 1 h at room temperature. In control experiments, the same concentration and volume of toxin solutions not containing oocytes were used. After incubation, 200 μL of the supernatant from each well was removed, spiked with 2-nitrophenol (2.5 μL of a 2.5 mg/mL solution in MilliQ water) that served as an internal standard, and 100 μL of this solution was subjected to HPLC by employing the same protocol that was used for the purification of DkTx and its variants (described on pg. 19 above). Fractional depletion was calculated as follows:

$$\text{Fraction depletion} = (R_{control}-R_{oocytes})/R_{control}$$

where $R_{control}$ is the averaged ratio of the area under the peak for the toxin and the area under the peak for 2-nitrophenol in the control experiments, and $R_{oocytes}$ is the ratio of the same parameters obtained from the oocyte samples (n = 3-5). Depletion assays on TRPV1-expressing oocytes (Figure S6b) were performed by using an identical protocol on oocytes injected with the TRPV1 cRNA 4 d earlier.

Figure S4. Interaction of wild-type DkTx and its variants with lipid membranes measured using tryptophan fluorescence. Tryptophan emission spectra of DkTx and its variants (left panel) in absence (dotted lines) and in presence (solid lines) of LUVs made from a 1:1 molar ratio of POPC: POPG. Relative fluorescence intensity (right panel) at 320 nm (F/F_0) as a function of the available lipid concentration (60% of total lipid concentration).Values of K_x of DkTx variants are provided in Table S2. Error bars correspond to SEM (n = 3 or 4).

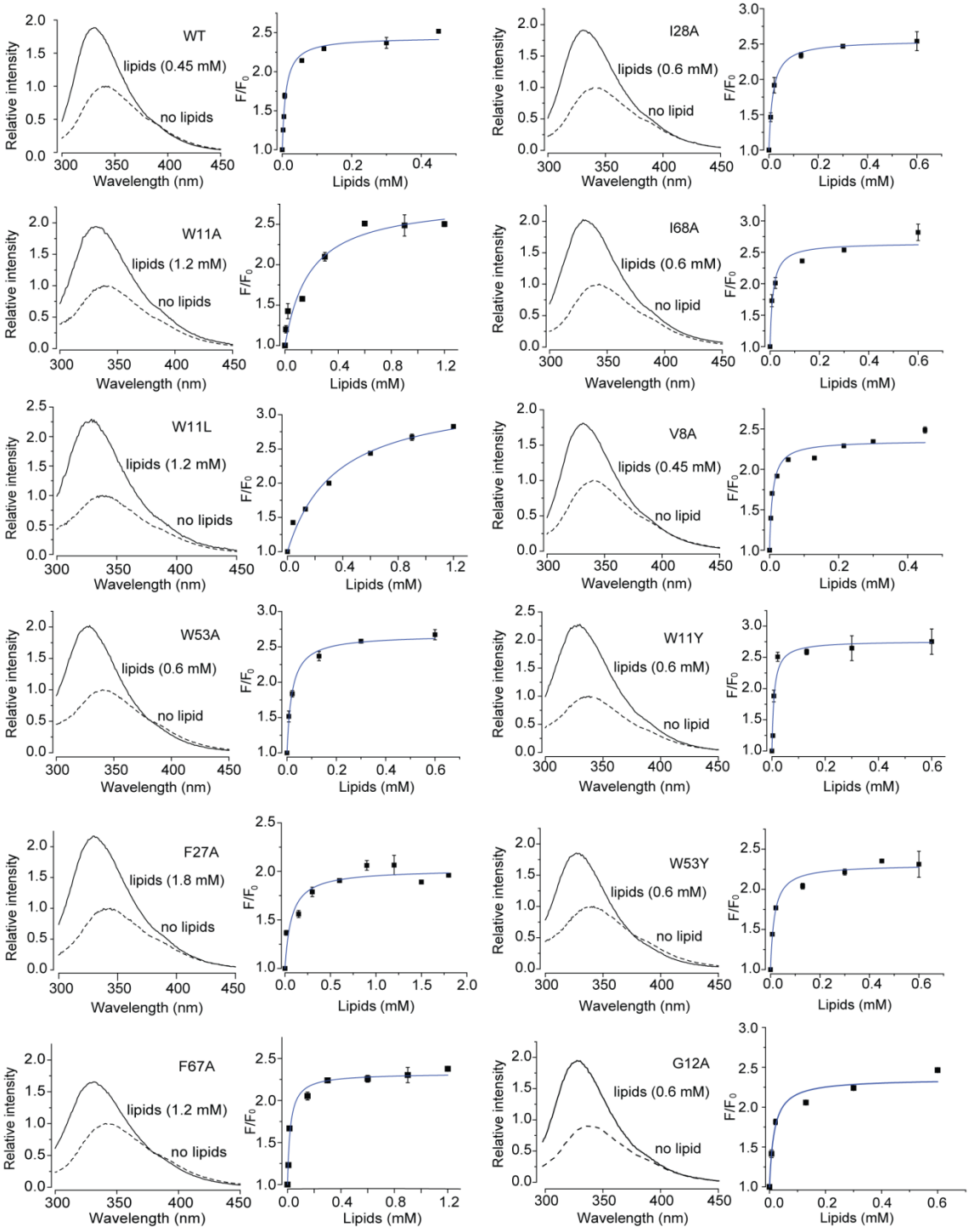

Figure S5. Mol. fraction partition coefficients of DkTx variants of K2 knot residues. Comparisons of mol. fraction partition coefficient (K_x) values of DkTx and its K2 variants. Error bars correspond to SEM (n = 3 or 4).

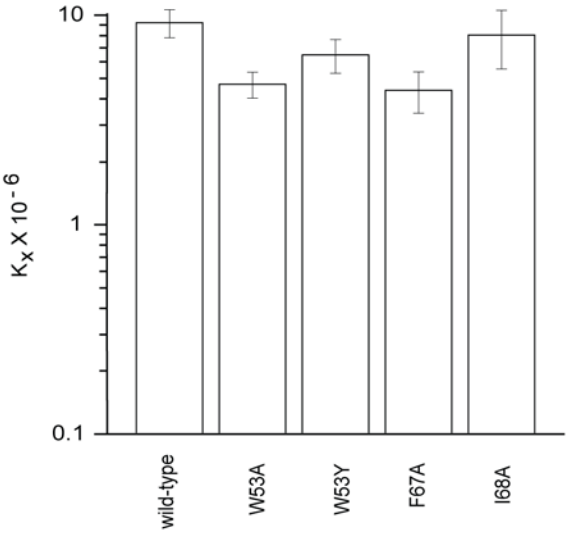

Figure S6. Toxin depletion assays performed with DkTx and its variants. a. Overlay of normalized HPLC chromatograms for toxin depletion experiments on DkTx variants on uninjected *Xenopus laevis* oocytes. Control traces are depicted in black and the experimental ones are depicted in red. **b.** Overlay chromatograms (left panel) for the depletion experiments performed with wild-type DkTx on uninjected and TRPV1-expressing oocytes. A bar graph depicting the fractional depletion obtained from the HPLC traces on the left panel is shown on the right panel. Error bars correspond to standard deviation values (n=3-5).

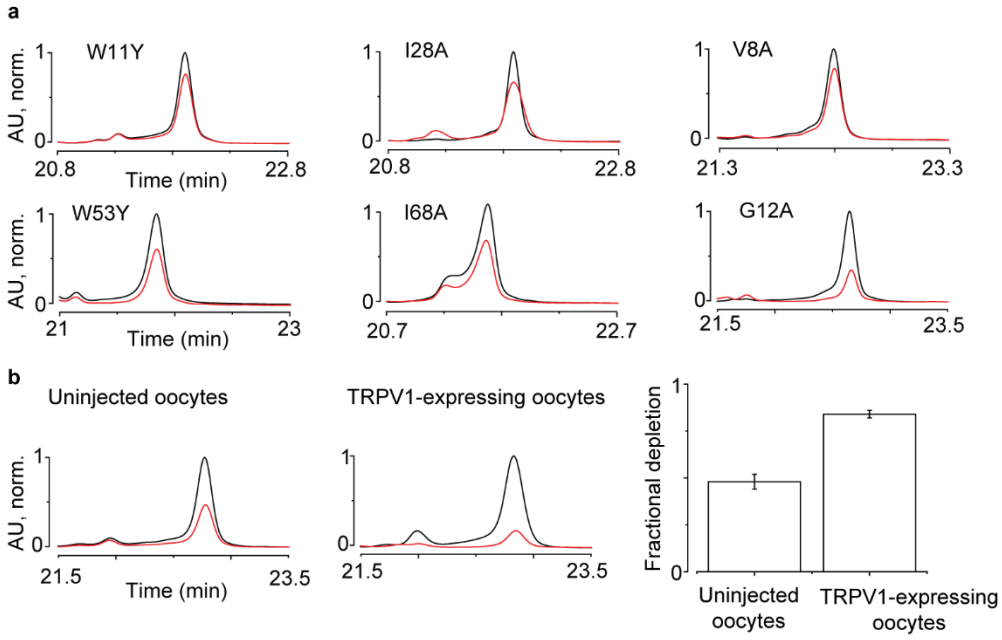

Table S2. Consolidated data summary for all DkTx variants

S. No.	Knot	DkTx variant	Expected mass (a.m.u.)	Observed mass (a.m.u.)	HPLC Retention time (min)	EC_{50} (μM)	Fold Change in EC_{50}	Hill Coefficient (n_H)	% Wash-off after 3 min of buffer perfusion post channel activation by saturation concentration of toxin	Mol. fraction partition coefficient (K_x)	Fractional depletion (oocytes)
1		Wild-type	9042.5	9043.1	22.4	0.14 ± 0.02	1.0	1.32 ± 0.17	33.77 ± 1.26 (1.1 μM)	(9.03±1.38)E6	0.48 ± 0.04
2	K1	D1A	8998.5	8995.3	24.4	0.08 ± 0.00	0.6	1.84 ± 0.22	25.81 ± 3.29 (0.55 μM)	N.D	N.D
3		E7A	8984.4	8982.5	22.3	1.59 ± 0.19	11.4	1.32 ± 0.17	25.97 ± 4.17 (13.2 μM)	N.D.	N.D
4		V8A	9014.4	9012.5	22.4	2.26 ± 0.15	16.1	1.13 ± 0.06	59.81 ± 0.69 (13.2 μM)	(1.06±0.21)E7	0.36 ± 0.01
5		S10A	9026.5	9027.7	22.4	0.22 ± 0.05	1.6	1.67 ± 0.38	12.13 ± 1.50 (1.1 μM)	N.D	N.D
6		W11A	8927.4	8925.0	21.6	11.22 ± 1.3	80.1	1.68 ± 0.17	95.30 ± 2.45 (26.4 μM)	(4.99±1.86)E5	0.20 ± 0.02
7		W11L	8969.4	8970.1	22.4	6.04 ± 2.01	43.1	1.54 ± 0.43	83.87 ± 5.10 (19.8 μM)	(2.63±0.57)E5	0.28 ± 0.03
8		W11Y	9019.4	9020.9	22.2	1.21 ± 0.04	8.6	1.41 ± 0.07	46.92 ± 2.70 (6.6 μM)	(1.1±0.4)E7	0.33 ± 0.01
9		G12A	9056.5	9055.6	22.9	1.08 ± 0.11	7.7	1.21 ± 0.16	68.91 ± 3.58 (13.2 μM)	(5.55±1.62)E6	0.62 ± 0.03
10		K13A	8985.4	8986.9	22.2	0.15 ± 0.02	1.1	1.01 ± 0.11	32.35 ± 5.32 (2.2 μM)	N.D	N.D
11		K14A	8985.4	8986.1	22.8	0.35 ± 0.07	2.5	1.26 ± 0.22	21.44 ± 3.63 (2.2 μM)	N.D	N.D
12		M25A	8982.4	8980.6	21.9	0.60 ± 0.13	4.3	0.96 ± 0.14	30.56 ± 6.10 (6.6 μM)	N.D	N.D
13		E26A	8984.4	8983.9	22.6	0.15 ± 0.03	1.1	1.31 ± 0.39	20.78 ± 3.03 (0.55 μM)	N.D	N.D
14		F27A	8966.4	8966.3	21.3	1.01 ± 0.02	7.2	2.14 ± 0.09	72.67± 5.78 (6.6 μM)	(1.29±0.61)E6	0.16 ±0.01
15		I28A	9000.4	9000.7	22.0	1.03 ± 0.13	7.4	1.22 ± 0.20	56.18 ± 5.90 (13.2 μM)	(5.74±0.4)E6	0.36 ±0.02
16		H30A	8976.4	8976.9	22.4	0.07 ± 0.00	0.5	2.12 ± 0.42	22.05 ± 5.45 (1.1 μM)	N.D	N.D
17	K2	N43A	8999.4	8998.9	22.4	0.25 ± 0.05	1.8	1.47 ± 0.27	42.94 ± 3.39 (1.1 μM)	N.D	N.D
18		V50A	9014.4	9014.8	22.1	2.44 ± 0.57	17.4	1.13 ±0.20	29.99 ± 2.93 (19.8 μM)	N.D.	N.D
19		G52A	9056.5	9056.0	22.3	0.62 ± 0.22	4.4	1.14 ± 0.34	41.06 ± 9.56 (6.6 μM)	N.D	N.D
20		W53A	8927.4	8926.2	21.2	N.A.	>100	N.A.	N.A.	(4.6±0.65)E6	0.49 ± 0.04
21		W53L	8969.4	8968.2	24.1	N.A.	>100	N.A.	N.A.	N.D	N.D
22		W53Y	9019.4	9021.4	22.1	1.11 ± 0.07	7.4	1.92 ± 0.22	33.12 ± 1.48 (6.6 μM)	(6.34±1.16)E6	0.42 ± 0.02
23		G54A	9056.5	9056.6	22.8	1.32 ± 0.37	9.4	0.99 ± 0.16	24.80 ± 3.07 (6.6 μM)	N.D	N.D
24		S55A	9026.5	9025.7	22.8	0.14 ± 0.01	1.0	1.24 ± 0.07	29.48 ± 3.72 (1.1 μM)	N.D	N.D
25		K56A	8985.4	8985.2	22.5	0.24 ± 0.01	1.7	1.55 ± 0.07	20.02 ± 6.66 (2.2 μM)	N.D	N.D
26		P64A	9016.4	9013.4	23.7	0.45 ± 0.05	3.2	2.30 ± 0.63	32.37 ± 2.83 (1.1 μM)	N.D	N.D
27		L65A	9000.4	9000.0	21.8	0.54 ± 0.11	3.9	1.05 ± 0.18	18.67 ± 7.73 (2.2 μM)	N.D	N.D
28		A66S	9058.4	9059.1	22.5	0.20 ± 0.02	1.4	1.25 ± 0.14	30.20 ± 5.13 (1.1 μM)	N.D	N.D
29		F67A	8966.4	8966.3	20.9	1.76 ± 0.23	12.6	1.59 ± 0.28	16.43 ± 5.20 (13.2 μM)	(4.30±0.95)E6	0.46 ± 0.04
30		I68A	9000.4	9002.1	21.3	0.64 ± 0.07	4.6	2.93 ± 0.98	27.15 ± 5.80 (6.6 μM)	(7.88±2.44)E6	0.5 ± 0.03
31		Y70A	8950.4	8950.3	22.6	0.11 ± 0.04	0.8	1.61 ± 0.83	36.75 ± 7.34 (0.55 μM)	N.D	N.D

Figure S7. a. Potency (EC_{50}) vs. mol. partitioning coefficient (K_x), and b. Potency (EC_{50}) vs. fractional depletion plots.

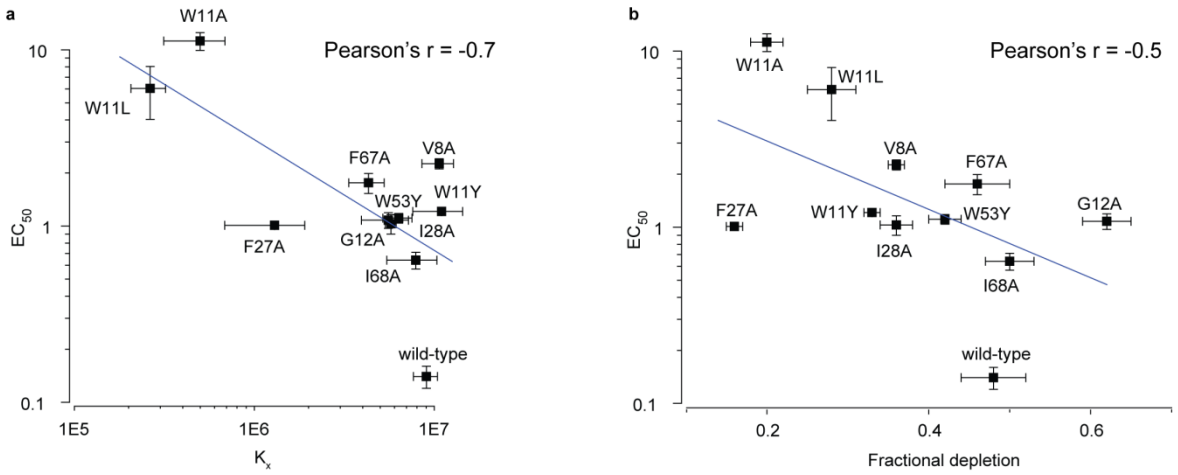

<u>Structural characterization of DkTx and its variants by Circular Dichroism (CD)</u>:

CD spectroscopic measurements were performed on a Jasco J-815 spectropolarimeter on protein solutions (50 µM) in sodium phosphate buffer (10 mM at pH 7.0) in a 0.1 cm cuvette at 25°C. Spectra obtained were reported as molar ellipticity [deg.cm^2/dmol]. Each representative spectra is an average of the 5 scans smoothened utilizing the Savitzky-Golay algorithm provided in the spectropolarimeter.

Figure S8. CD spectra of DkTx and its variants.

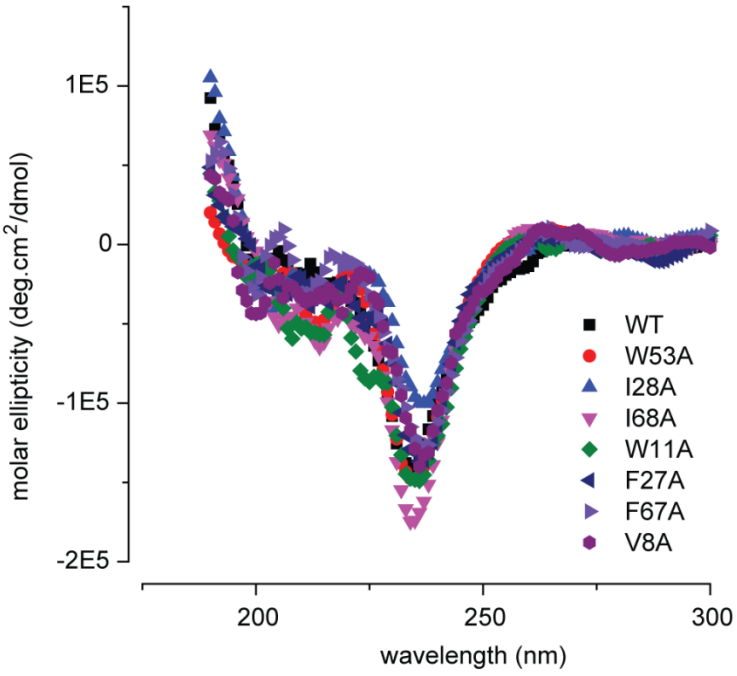

References:

1. Gao, Y., Cao, E., Julius, D., and Cheng, Y. (2016) TRPV1 structures in nanodiscs reveal mechanisms of ligand and lipid action, *Nature* 534, 347-351.

2. Bae, C., Anselmi, C., Kalia, J., Jara-Oseguera, A., Schwieters, C. D., Krepkiy, D., Won Lee, C., Kim, E. H., Kim, J. I., Faraldo-Gomez, J. D., and Swartz, K. J. (2016) Structural insights into the mechanism of activation of the TRPV1 channel by a membrane-bound tarantula toxin, *eLife 5*, e11273.

3. Bae, C., Kalia, J., Song, I., Yu, J., Kim, H. H., Swartz, K. J., and Kim, J. I. (2012) High yield production and refolding of the double-knot toxin, an activator of TRPV1 channels, *PLoS One 7*, e51516.

4. Gupta, K., Zamanian, M., Bae, C., Milescu, M., Krepkiy, D., Tilley, D. C., Sack, J. T., Yarov-Yarovoy, V., Kim, J. I., and Swartz, K. J. (2015) Tarantula toxins use common surfaces for interacting with Kv and ASIC ion channels, *eLife 4*, e06774.

5. Ladokhin, A.S., Jayasinghe, S., and White, S.H (2000) How to Measure and Analyze Tryptophan Fluorescence in Membranes Properly, and Why Bother? *Anal Biochem* 285, 235-245.